INTERNATIONAL JOURNAL FOR NUMERICAL METHODS IN FLUIDS
Int. J. Numer. Meth. Fluids 2002; **39**:1001–1011 (DOI: 10.1002/fld.358)

On the quadrilateral Q_2–P_1 element for the Stokes problem

Daniele Boffi[1,*,†] and Lucia Gastaldi[2,‡]

[1] *Dipartimento di Matematica, Università di Pavia, 27100 Pavia, Italy*
[2] *Dipartimento di Matematica, Università di Brescia, 25133 Brescia, Italy*

SUMMARY

The $Q_2 - P_1$ approximation is one of the most popular Stokes elements. *Two* possible choices are given for the definition of the pressure space: one can either use a *global* pressure approximation (that is on each quadrilateral the finite element space is spanned by 1 and by the global co-ordinates x and y) or a *local* approach (consisting in generating the local space by means of the constants and the local curvilinear co-ordinates on each quadrilateral ξ and η). The *former* choice is known to provide *optimal error* estimates on general meshes. This has been shown, as it is standard, by proving a discrete inf–sup condition. In the present paper we check that the *latter* approach satisfies the inf–sup condition as well. However, recent results on quadrilateral finite elements bring to light a *lack* in the approximation properties for the space coming out from the *local* pressure approach. Numerical results actually show that the second choice (local or *mapped* pressure approximation) is *suboptimally* convergent. Copyright © 2002 John Wiley & Sons, Ltd.

KEY WORDS: Stokes problem; mixed finite elements; quadrilateral

1. INTRODUCTION

In this paper we shall deal with the Q_2–P_1 mixed finite element approximation of the Stokes problem in a polygonal domain Ω: given f find $\underline{u}$ and p such that

$$\begin{aligned} -\underline{\Delta u} + \nabla p &= \underline{f} \quad \text{in } \Omega \\ \operatorname{div} \underline{u} &= 0 \quad \text{in } \Omega \\ \underline{u} &= 0 \quad \text{on } \partial\Omega \end{aligned} \tag{1}$$

A standard variational formulation is given by

$$L_0^2(\Omega) = \left\{ v : \Omega \to \mathbb{R} \,\middle|\, \int_\Omega v^2 < +\infty, \int_\Omega v = 0 \right\}$$

* Correspondence to: D. Boffi, Dipartimento di Matematica, Università di Pavia, 27100 Pavia, Italy.
† E-mail: boffi@dimat.unipv.it, *URL*: http://dimat.unipv.it/~boffi/.
‡ E-mail: gastaldi@bsing.ing.unibs.it, *URL*: http://bsing.ing.unibs.it/~gastaldi/.

Received 15 December 2000
Revised 25 February 2002

$$\begin{aligned} H_0^1(\Omega) &= \left\{ v:\Omega\to\mathbb{R} \,\middle|\, \int_\Omega |\nabla v|^2 < +\infty,\ v=0 \text{ on } \partial\Omega \right\} \\ V &= H_0^1(\Omega)^2 \\ Q &= L_0^2(\Omega) \end{aligned} \tag{2}$$

given $f\in V'$ find $(\underline{u},p)\in V\times Q$ such that

$$\begin{aligned} (\underline{\underline{\nabla}}\underline{u}, \underline{\underline{\nabla}}\underline{v}) - (\operatorname{div}\underline{v}, p) &= \langle \underline{f}, \underline{v}\rangle \quad \forall \underline{v}\in V \\ (\operatorname{div}\underline{u}, q) &= 0 \qquad\quad\ \forall q\in Q \end{aligned}$$

where $(\cdot,\cdot)$ denotes the scalar product in $L^2(\Omega)^n$ $(n=1,2)$ and $\langle\cdot,\cdot\rangle$ the duality pair between V and V'.

It is classical to build a conforming finite element approximation of Equation (2) by choosing finite dimensional subspaces $V_h\subset V$ and $Q_h\subset Q$ and to consider the following discrete problem:

find $(\underline{u}_h, p_h)\in V_h\times Q_h$ such that

$$\begin{aligned} (\underline{\underline{\nabla}}\underline{u}_h, \underline{\underline{\nabla}}\underline{v}) - (\operatorname{div}\underline{v}, p_h) &= \langle \underline{f}, \underline{v}\rangle \quad \forall \underline{v}\in V_h \\ (\operatorname{div}\underline{u}_h, q) &= 0 \qquad\quad\ \forall q\in Q_h \end{aligned} \tag{3}$$

The standard theory of mixed finite elements [1] states that the inf–sup condition

$$\exists\beta>0 \quad \text{s.t.} \sup_{\underline{v}\in V_h} \frac{(\operatorname{div}\underline{v}, q)}{\|\underline{v}\|_V} \geqslant \beta\|q\|_Q, \quad \forall q\in Q_h \tag{4}$$

implies the following estimate

$$\|\underline{u}-\underline{u}_h\|_V + \|p-p_h\|_Q \leqslant C \inf_{\underline{v}\in V_h, q\in Q_h} (\|\underline{u}-\underline{v}\|_V + \|p-q\|_Q) \tag{5}$$

with C independent of h.

Let us consider separately the two terms in the right-hand side of estimate (5) when using the Q_2–P_1 scheme.

To make the definitions of the discrete spaces clearer, we introduce some notation. We shall denote by $\hat{K}$ the reference square, by K a generic quadrilateral and by $F_K:\hat{K}\to K$ the bilinear mapping associated with K. The global co-ordinates on $\hat{K}$ will be denoted by $(\hat{x},\hat{y})$, while the co-ordinates on K by (x,y).

We approximate the velocity space V by means of continuous piecewise biquadratic vector fields, i.e. $V_h=\mathcal{Q}_2\cap H_0^1(\Omega)^2$. This means that on the reference square $\hat{K}$ each component of the shape functions is the tensor product of a quadratic polynomial in x and a quadratic polynomial in y, that is

$$\underline{\hat{\varphi}}(\hat{x},\hat{y}) = \left(\sum_{i,j=0}^{2} a_{ij}\hat{x}^i\hat{y}^j, \sum_{i,j=0}^{2} b_{ij}\hat{x}^i\hat{y}^j \right)$$

We then define the shape functions on the physical element K by composing $\underline{\hat{\varphi}}$ with the inverse of the mapping F_K, namely

$$\underline{\varphi}(x,y) = \underline{\hat{\varphi}}(F_K^{-1}(x,y))$$

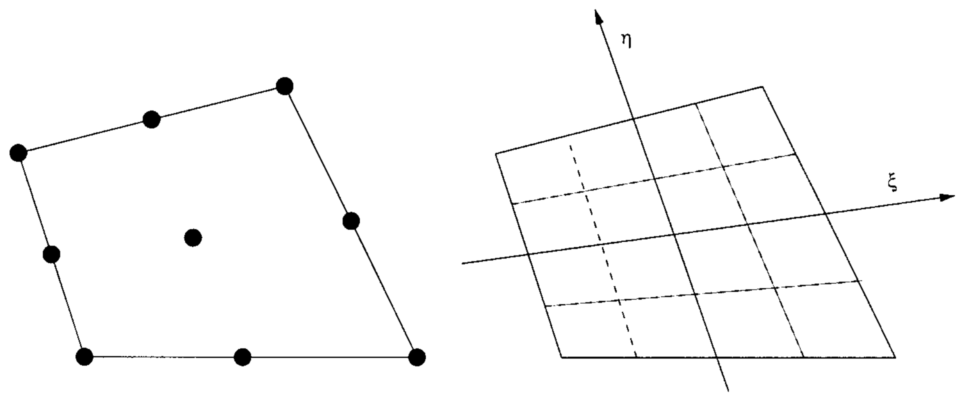

Figure 1. The space V_h and the local co-ordinate frame (ξ, η).

Another equivalent way of presenting the space V_h is to introduce a local *curvilinear* co-ordinate frame on K, usually denoted by (ξ, η), and to define the shape functions locally as

$$\underline{\varphi}(\xi,\eta) = \left(\sum_{i,j=0}^{2} a_{ij} \xi^i \eta^j, \sum_{i,j=0}^{2} b_{ij} \xi^i \eta^j \right)$$

In Figure 1 the degrees of freedom for V_h are plotted together with the local co-ordinate system (ξ, η).

Standard finite element approximation properties state that the bound

$$\inf_{\underline{v} \in V_h} \|\underline{u} - \underline{v}\|_V = O(h^2) \tag{6}$$

holds true provided the triangulation sequence is regular and the solution $\underline{u}$ is smooth enough.

On the other hand, two choices are possible for the definition of Q_h.

C1: the first one consists in defining Q_h the same way as we did for the space V_h, that is locally spanned by 1, ξ and η. The construction can be presented in two possible ways:

- either considering a shape function

  $$\hat{\psi}(\hat{x}, \hat{y}) = a_0 + a_1 \hat{x} + a_2 \hat{y}$$

  defined on the reference square $\hat{K}$ and then transforming it using the mapping F_k as follows:

  $$\psi(x, y) = \hat{\psi}(F_K^{-1}(x, y))$$

- or making use of the local co-ordinates, namely

  $$\psi(\xi, \eta) = a_0 + a_1 \xi + a_2 \eta$$

C2: the second possible choice consists in using *unmapped* linear functions, that is

$$\psi(x, y) = a_0 + a_1 x + a_2 y$$

We remark that choice C2 was not possible for the definition of V_h: without the use of the mapping F_K it turns out that no continuity can be imposed from one element to the other. On the other hand functions in Q_h need not be continuous, so that this choice is practicable in this case.

Recent results show that choice C2 is actually the correct one for what the approximation properties are concerned. Let us call $Q^{(i)}$, $i=1,2$ the discrete spaces obtained by means of choice Ci. In Reference [2] it has been proved that

$$\begin{aligned}\inf_{q\in Q^{(1)}} \|p-q\|_Q &= O(h)\\ \inf_{q\in Q^{(2)}} \|p-q\|_Q &= O(h^2)\end{aligned} \tag{7}$$

when the mesh sequence is regular and the solution p is smooth enough. Actually, the second bound in Equation (7) is not new, while the first one is suboptimal and can be made more precise. In particular in Reference [2] a sequence of meshes of a square has been presented for which the first bound in Equation (7) cannot be improved even if p is a polynomial.

The results presented so far imply that if one is interested in an optimal approximation of the solution $(\underline{u}, p)$ of the Stokes problem (1) by means of the Q_2–P_1 method then one necessarily has to use $Q_h = Q^{(2)}$, that is a global (or unmapped) pressure approach. Numerical evidence of this pathology has been reported with no explanation in a particular case also in Reference [3].

According to Reference [1, p.216] the inf–sup condition (4) in the case $Q_h = Q^{(2)}$ has been proven first in 1979 during the Banff Conference on Finite Elements in Flow Problems. Two different proofs can be found in References [4, 5]. Hence the following bounds are achieved for the global approach, provided $\underline{u}$ and p are regular enough:

$$\|\underline{u}-\underline{u}_h\|_V + \|p-p_h\|_Q = O(h^2) \tag{8}$$

On the other hand, the choice $Q_h = Q^{(1)}$, that is a local (or mapped) approach has never been analysed from the mathematical point of view even if it has been used sometimes by the practitioners. The aim of this paper is to show that the local approach *is never* to be used even if one is only interested in the first component $\underline{u}$ of the solution of (2). In order to do that, we first prove that the $V_h - Q^{(1)}$ method is a good mixed method, in the sense that the inf–sup condition (4) is satisfied. The proof of this result is given in Section 2, together with a recap on the macroelement technique by Stenberg [5].

The stability of the choice $Q_h = Q^{(1)}$, together with (5), (6) and the first of (7) gives a V_h-suboptimal bound

$$\|\underline{u}-\underline{u}_h\|_V + \|p-p_h\|_Q = O(h) \tag{9}$$

even for smooth $\underline{u}$ and p.

One could think, however, that the discrete velocity $\underline{u}_h$ behaves better than estimate (9) says and that the local method might be used if one is not interested in a good approximation of p.

In Section 3 we report on our numerical experiments which confirm the general behaviour of mixed approximations: with $Q_h = Q^{(1)}$ estimate (9) cannot be improved in general. In particular, using the sequence of meshes introduced in Reference [2], with a particular choice of $\underline{f}$ (which is a polynomial, so that no regularity issue is present in our example), we find that $\|\underline{u} - \underline{u}_h\|_V$ is nothing better than $O(h)$.

2. THE INF–SUP CONDITION

For the proof of the inf–sup condition we shall apply the macroelement technique.

We shall make use of the following notation. A *macroelement* is an open polygon, which is the union of adjacent elements. A macroelement M is said to be *equivalent* to a reference element $\hat{M}$ if there exists a mapping $F_M : \hat{M} \rightarrow M$ such that

(1) F_M is continuous and invertible;
(2) $F_M(\hat{M}) = M$;
(3) If $\hat{M} = \bigcup \hat{K}_j$, where $\hat{K}_j$, $j = 1, \ldots, m$ are the elements defining $\hat{M}$, then $K_j = F_M(\hat{K}_j)$, $j = 1, \ldots, m$, are the elements of M;
(4) $F_M|_{\hat{K}_j} = F_{\hat{K}_j} \circ F_{K_j}^{-1}$, $j = 1, \ldots, m$, where we recall that F_K denotes the bilinear mapping from the reference element to the generic element K.

We denote by $\mathscr{E}_{\hat{M}}$ the equivalence class of $\hat{M}$. We now introduce the discrete spaces associated with V_h and Q_h on the generic macroelement M.

$$V_{0,M} = \{\underline{v} \in H_0^1(M)^2 | \underline{v} = \underline{w}|_M \text{ with } \underline{w} \in V_h\}$$

$$Q_{0,M} = \left\{ p \in L^2(\Omega) \,\middle|\, \int_M p = 0, \;\; p = q|_M \text{ with } q \in Q_h \right\}$$

We finally introduce a space which corresponds to the kernel of the transpose of the discrete divergence operator acting on $V_{0,M}$.

$$K_M = \left\{ p \in Q_{0,M} \,\middle|\, \int_M p \operatorname{div} \underline{v} = 0, \;\; \forall \underline{v} \in V_{0,M} \right\}$$

The *macroelement condition* reads

$$K_M = \{0\} \tag{10}$$

We shall use the following macroelement lemma which follows from the theory in Reference [3]:

Lemma 1
Suppose that each triangulation can be decomposed in disjoint macroelements belonging to a *fixed* number (independent of h) of equivalence classes $\mathscr{E}_{\hat{M}_i}$, $i = 1, \ldots, n$. Suppose, moreover, that V_h is such that the pair $V_h - K_h$ satisfies the inf–sup condition (4), where K_h is the space of piecewise constant functions contained in Q. Then the macroelement condition (10) (for every $M \in \mathscr{E}_{\hat{M}_i}$, $i = 1, \ldots, n$) implies the inf–sup condition (4) for the spaces $V_h - Q_h$.

The next theorem is the main result of this section.

Theorem 1
Let V_h be defined as in the introduction (i.e. $V_h = \mathscr{Q}_2 \cap H_0^1(\Omega)^2$) and Q_h be like in choice C1 (that is piecewise linear functions with the local or mapped approach). Then the inf–sup condition (4) holds true.

Proof
We use the macroelement technique with macroelements consisting of only one element. We then prove that the macroelement condition (10) is satisfied with $M = K$ for any element K of our mesh.

Let us denote by $\underline{v}_1$ and $\underline{v}_2$ the basis functions associated to the node internal to K (with the notation above, $V_{0,K}$ is spanned by $\{\underline{v}_1, \underline{v}_2\}$). Moreover, we shall denote by ξ and η the two components of the inverse of F_K, that is, $Q_{0,K}$ is spanned by $\{\xi - \xi_0, \eta - \eta_0\}$, where ξ_0 and η_0 are the averages on K of ξ and η, respectively.

The macroelement condition (10) reduces to an algebraic problem. Namely, we are led to show that the matrix

$$B_K = \begin{pmatrix} \displaystyle\int_K \operatorname{div} \underline{v}_1 \xi \, \mathrm{d}x \, \mathrm{d}y & \displaystyle\int_K \operatorname{div} \underline{v}_1 \eta \, \mathrm{d}x \, \mathrm{d}y \\ \displaystyle\int_K \operatorname{div} \underline{v}_2 \xi \, \mathrm{d}x \, \mathrm{d}y & \displaystyle\int_K \operatorname{div} \underline{v}_2 \eta \, \mathrm{d}x \, \mathrm{d}y \end{pmatrix}$$

is non-singular.

If $\hat{K}$ is the reference square $]-1,1[\times]-1,1[$ and the bilinear mapping $F_K : \hat{K} \to K$ is given by

$$\begin{aligned} x &= a_1 + a_2\hat{x} + a_3\hat{y} + a_4\hat{x}\hat{y} \\ y &= b_1 + b_2\hat{x} + b_3\hat{y} + b_4\hat{x}\hat{y} \end{aligned} \tag{11}$$

then the jacobian matrix is

$$J(\hat{x}, \hat{y}) = \begin{pmatrix} a_2 + a_4\hat{y} & a_3 + a_4\hat{x} \\ b_2 + b_4\hat{y} & b_3 + b_4\hat{x} \end{pmatrix} \tag{12}$$

On the reference square $\hat{K}$ the basis functions associated with the internal node (0,0) are:

$$\hat{\underline{v}}_1 = \begin{pmatrix} \varphi \\ 0 \end{pmatrix}, \quad \hat{\underline{v}}_2 = \begin{pmatrix} 0 \\ \varphi \end{pmatrix} \tag{13}$$

where $\varphi(\hat{x}, \hat{y}) = (1 - \hat{x}^2)(1 - \hat{y}^2)$. By simple calculation we obtain

$$B_K = \frac{16}{9} \begin{pmatrix} -b_3 & b_2 \\ a_3 & -a_2 \end{pmatrix}$$

Hence B_K is not singular if and only if $b_3a_2 - a_3b_2 \neq 0$. On the other hand, we see that $\det J(0,0) = b_3a_2 - a_3b_2$, and this must be non-zero, since we know that $\det J(\hat{x}, \hat{y})$ is different from zero for all $(\hat{x}, \hat{y}) \in \hat{K}$. □

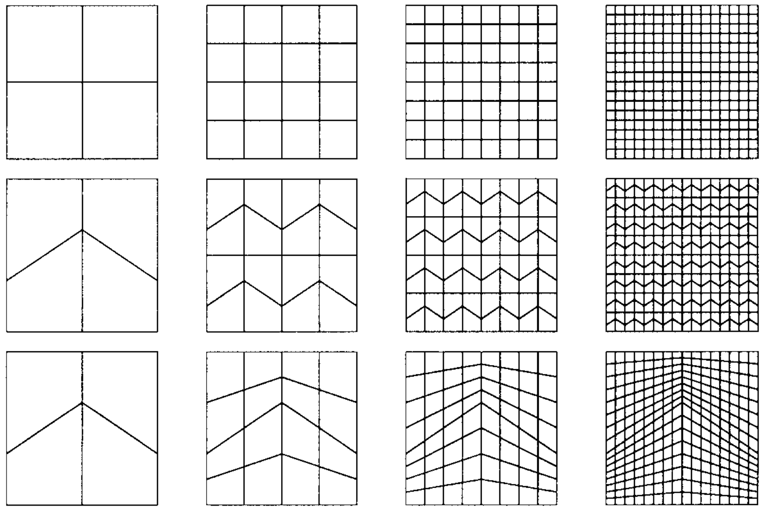

Figure 2. Three sequences of meshes of the unit square: square, trapezoidal, and asymptotically parallelogram. Each is shown for $n = 2, 4, 8$, and 16.

3. NUMERICAL RESULTS

In this section we report on the results of numerical experiments which confirm that the use of the choice C2 (i.e. global unmapped linears) is to be preferred with respect to choice C1 (local mapped linears).

In our first test we consider the Stokes problem (1) with $\Omega =]0,1[^2$ and an RHS $\underline{f}$ such that the exact solution $(\underline{u}, p)$ is given by

$$\begin{aligned} u_1 &= -2x^2y(1-x)^2(1-3y+2y^2) \\ u_2 &= 2xy^2(1-y)^2(1-3x+2x^2) \\ p &= x+y-1 \end{aligned}$$

Notice that p is a linear function, so that we might expect some superconvergence properties.

We introduce three sequences of meshes, according to the numerical experiments presented in Reference [2] (see Figure 2). The first sequence is a standard uniform partition of the square in n^2 subsquares. Each mesh of the second sequence is composed of self-similar trapezoids in such a way that the distortion of the mesh is kept constant as h goes to zero. Finally, the last sequence is built up with *asymptotically parallel* quadrilaterals, that is the elements tend to become parallelograms as h goes to zero.

As it was expected, in the case of the mesh of squares the two methods are equivalent (even though the corresponding matrices are not the same; they depend on the chosen basis for Q_h). In Table I it is shown how the velocities converge with the correct rate (second order in the H^1 norm and third order in L^2) while the pressure superconverges with order 3 instead of 2 in L^2.

Table I. Errors and rates of convergence for the test problem with square mesh.

n	$\|\underline{u}-\underline{u}_h\|_{L^2}$			$\|\underline{\underline{\nabla}}(\underline{u}-\underline{u}_h)\|_{L^2}$			$\|p-p_h\|_{L^2}$		
	Err.	(%)	Rate	Err.	(%)	Rate	Err.	(%)	Rate
Mapped biquadratic—mapped linear element									
2	8.3e − 04	15.134		9.0e − 03	35.621		1.0e − 02	0.954	
4	1.2e − 04	2.179	2.8	2.3e − 03	13.534	1.4	1.3e − 03	0.119	3.0
8	1.5e − 05	0.276	3.0	5.6e − 04	2.251	2.6	1.7e − 04	0.016	2.9
16	1.9e − 06	0.034	3.0	1.4e − 04	0.561	2.0	2.1e − 05	0.002	3.0
32	2.4e − 07	0.004	3.0	3.5e − 05	0.140	2.0	2.6e − 06	0.000	3.2
Mapped biquadratic—unmapped linear element									
2	8.3e − 04	15.134		9.0e − 03	35.621		1.0e − 02	0.954	
4	1.2e − 04	2.179	2.8	2.3e − 03	13.534	1.4	1.3e − 03	0.119	3.0
8	1.5e − 05	0.276	3.0	5.6e − 04	2.251	2.6	1.7e − 04	0.016	2.9
16	1.9e − 06	0.034	3.0	1.4e − 04	0.561	2.0	2.1e − 05	0.002	3.0
32	2.4e − 07	0.004	3.0	3.5e − 05	0.140	2.0	2.6e − 06	0.000	3.2

Table II. Errors and rates of convergence for the test problem with uniform trapezoid mesh.

n	$\|\underline{u}-\underline{u}_h\|_{L^2}$			$\|\underline{\underline{\nabla}}(\underline{u}-\underline{u}_h)\|_{L^2}$			$\|p-p_h\|_{L^2}$		
	Err.	(%)	Rate	Err.	(%)	Rate	Err.	(%)	Rate
Mapped biquadratic—mapped linear element									
2	1.4e − 03	25.438		1.3e − 02	52.071		1.6e − 01	15.060	
4	4.0e − 04	7.341	1.7	6.2e − 03	24.541	1.1	9.1e − 02	8.395	0.8
8	1.1e − 04	1.991	1.9	3.0e − 03	12.218	1.0	3.9e − 02	3.606	1.2
16	2.9e − 05	0.524	1.9	1.5e − 03	6.248	1.0	1.8e − 02	1.685	1.1
32	7.4e − 06	0.134	2.0	7.8e − 04	3.177	1.0	9.0e − 03	0.836	1.0
Mapped biquadratic—unmapped linear element									
2	1.2e − 03	21.064		1.2e − 02	44.026		1.2e − 02	3.066	
4	1.8e − 04	3.335	2.6	3.3e − 03	13.170	1.7	3.3e − 03	0.805	1.9
8	2.2e − 05	0.405	3.0	8.3e − 04	3.319	2.0	5.5e − 04	0.134	2.6
16	2.8e − 06	0.050	3.0	2.1e − 04	0.836	2.0	1.2e − 04	0.029	2.2
32	3.5e − 07	0.006	3.0	5.2e − 05	0.209	2.0	2.6e − 05	0.006	2.2

For the second sequence of meshes the behaviour is completely different (see Table II). If the pressure space is chosen locally (mapped pressures) then the suboptimality of the method is evident: only first order in the energy norm. On the other hand with the correct global choice (unmapped pressures) then one recovers the optimal second order accuracy.

Finally, with the asymptotically affine mesh we have results comparable with the ones obtained with the mesh of squares (see Table III).

Our second test is a slight variant of the first one: $\underline{f}$ is chosen in such a way that the first component of the solution $\underline{u}$ is still the same polynomial as before, while the pressure is given by

$$p(x,y) = \cos(\pi x)\cos(\pi y)$$

Table III. Errors and rates of convergence for the test problem with asymptotically parallelogram mesh.

n	$\Vert\underline{u}-\underline{u}_h\Vert_{L^2}$			$\Vert\underline{\nabla}(\underline{u}-\underline{u}_h)\Vert_{L^2}$			$\Vert p-p_h\Vert_{L^2}$		
	Err.	(%)	Rate	Err.	(%)	Rate	Err.	(%)	Rate
Mapped biquadratic—mapped linear element									
2	1.4e − 03	25.438		1.3e − 02	52.071		1.6e − 01	15.060	
4	1.9e − 04	3.515	2.8	3.5e − 03	14.080	1.9	2.6e − 02	2.452	2.6
8	2.3e − 05	0.414	3.1	8.3e − 04	3.351	2.1	6.0e − 03	0.556	2.1
16	2.8e − 06	0.050	3.0	2.0e − 04	0.801	2.1	1.4e − 03	0.132	2.1
32	3.4e − 07	0.006	3.0	4.8e − 05	0.195	2.0	3.5e − 04	0.032	2.0
Mapped biquadratic—unmapped linear element									
2	1.2e − 03	21.064		1.2e − 02	44.026		1.2e − 02	3.066	
4	1.7e − 04	3.076	2.8	3.0e − 03	11.983	1.9	2.1e − 03	0.512	2.6
8	2.1e − 05	0.391	3.0	7.6e − 04	3.018	2.0	2.6e − 04	0.064	3.0
16	2.7e − 06	0.049	3.0	1.9e − 04	0.755	2.0	3.2e − 05	0.008	3.0
32	3.4e − 07	0.006	3.0	4.7e − 05	0.189	2.0	3.9e − 06	0.001	3.0

Table IV. Errors and rates of convergence for the test problem with square mesh.

n	$\Vert\underline{u}-\underline{u}_h\Vert_{L^2}$			$\Vert\underline{\nabla}(\underline{u}-\underline{u}_h)\Vert_{L^2}$			$\Vert p-p_h\Vert_{L^2}$		
	Err.	(%)	Rate	Err.	(%)	Rate	Err.	(%)	Rate
Mapped biquadratic—mapped linear element									
2	8.3e − 04	15.134		9.0e − 03	35.622		1.3e − 01	25.646	
4	2.5e − 04	4.513	1.7	5.1e − 03	20.764	0.8	3.1e − 02	6.144	2.1
8	2.1e − 05	0.386	3.5	9.2e − 04	3.717	2.5	7.6e − 03	1.528	2.0
16	2.1e − 06	0.039	3.3	1.7e − 04	0.689	2.4	1.9e − 03	0.381	2.0
32	2.5e − 07	0.005	3.1	3.7e − 05	0.149	2.2	4.8e − 04	0.095	2.0
Mapped biquadratic—unmapped linear element									
2	8.3e − 04	15.134		9.0e − 03	35.622		1.3e − 01	25.646	
4	2.5e − 04	4.513	1.7	5.1e − 03	20.764	0.8	3.1e − 02	6.144	2.0
8	2.1e − 05	0.386	3.5	9.2e − 04	3.717	2.5	7.6e − 03	1.528	2.0
16	2.1e − 06	0.039	3.3	1.7e − 04	0.689	2.4	1.9e − 03	0.381	2.0
32	2.5e − 07	0.004	3.1	3.7e − 05	0.149	2.2	4.8e − 04	0.095	2.0

In this case p is not a linear function and we do not expect any superconvergence. In Tables IV–VI we show the results obtained using the three sequences of meshes presented in Figure 2.

4. CONCLUSIONS

In this paper we considered two possible versions of the Q_2–P_1 Stokes element. They are characterized by two different definitions of the space of pressures: the *global* (unmapped) approach and the *local* (mapped) scheme. The former was known to satisfy the inf–sup condition, while for the latter a new proof is proposed which makes use of the macroelement technique.

Table V. Errors and rates of convergence for the test problem with uniform trapezoid mesh.

n	$\Vert\underline{u}-\underline{u}_h\Vert_{L^2}$			$\Vert\underline{\nabla}(\underline{u}-\underline{u}_h)\Vert_{L^2}$			$\Vert p-p_h\Vert_{L^2}$		
	Err.	(%)	Rate	Err.	(%)	Rate	Err.	(%)	Rate
Mapped biquadratic—mapped linear element									
2	2.4e − 03	43.203		2.3e − 02	92.918		1.6e − 01	32.567	
4	6.2e − 04	11.214	1.9	1.0e − 02	39.691	1.2	4.1e − 02	8.207	2.0
8	1.7e − 04	3.063	1.9	4.8e − 03	19.366	1.0	1.4e − 02	2.777	1.6
16	4.5e − 05	0.811	1.9	2.4e − 03	9.842	1.0	5.8e − 03	1.166	1.3
32	1.1e − 05	0.209	2.0	1.2e − 03	4.996	1.0	2.8e − 03	0.550	1.1
Mapped biquadratic—unmapped linear element									
2	1.6e − 03	29.542		1.6e − 02	64.059		1.5e − 01	30.410	
4	3.2e − 04	5.753	2.4	6.2e − 03	24.529	1.4	3.5e − 02	6.984	2.1
8	3.8e − 05	0.694	3.1	1.5e − 03	6.144	2.0	8.6e − 03	1.720	2.0
16	4.6e − 06	0.084	3.0	3.7e − 04	1.492	2.0	2.2e − 03	0.429	2.0
32	5.7e − 07	0.010	3.0	4.6e − 05	0.370	2.0	1.0e − 04	0.107	2.0

Table VI. Errors and rates of convergence for the test problem with asymptotically parallelogram mesh.

n	$\Vert\underline{u}-\underline{u}_h\Vert_{L^2}$			$\Vert\underline{\nabla}(\underline{u}-\underline{u}_h)\Vert_{L^2}$			$\Vert p-p_h\Vert_{L^2}$		
	Err.	(%)	Rate	Err.	(%)	Rate	Err.	(%)	Rate
Mapped biquadratic—mapped linear element									
2	2.4e − 03	43.203		2.3e − 02	92.918		1.6e − 01	32.567	
4	4.1e − 04	7.426	2.5	7.5e − 03	30.198	1.6	3.9e − 02	7.709	2.0
8	3.6e − 05	0.663	3.5	1.5e − 03	6.093	2.3	9.7e − 03	1.933	2.0
16	3.5e − 06	0.063	3.4	2.9e − 04	1.146	2.4	2.4e − 03	0.481	2.0
32	3.8e − 07	0.007	3.2	5.9e − 05	0.235	2.3	6.0e − 04	0.120	2.0
Mapped biquadratic—unmapped linear element									
2	1.6e − 03	29.542		1.6e − 02	64.059		1.5e − 01	30.410	
4	3.6e − 04	6.591	2.2	6.9e − 03	27.851	1.2	3.5e − 02	7.048	2.1
8	3.4e − 05	0.618	3.4	1.4e − 03	5.633	2.3	8.9e − 03	1.777	2.0
16	3.4e − 06	0.061	3.3	2.7e − 04	1.076	2.4	2.2e − 03	0.444	2.0
32	3.7e − 07	0.007	3.2	5.7e − 05	0.226	2.3	5.5e − 04	0.111	2.0

Theoretical results presented in Reference [2] imply that the *local* pressure method *cannot be* second order accurate in the case of *general* quadrilateral meshes because of a lack in the approximation properties of mapped linear finite elements. Our numerical tests *confirm* this result *and* show that the velocities are suboptimally convergent too. This is in agreement with the standard estimates of mixed finite elements in which the primal and the dual variables are linked together.

On the other hand, the numerical experiments for the global pressure approach show *the theoretically proven optimal convergence*.

The local pressure approach, however, behaves correctly if one uses a mesh of parallelograms *or a* sequence of meshes for which the elements tend to become parallelograms.

REFERENCES

1. Brezzi F, Fortin M. *Mixed and Hybrid Finite Element Methods*. Springer: New York, 1991.
2. Arnold DN, Boffi D, Falk RS. Approximation by quadrilateral finite elements. *Mathematics of Computation* 2002; **71**:909–922.
3. Gresho P, Sani R, Engelman MS. *Incompressible Flow and the Finite Element Method Advection–Diffusion and Isothermal Laminar Flow*. Wiley: West Sussex, UK, 1998.
4. Girault V, Raviart P-A. *Finite Element Methods for Navier–Stokes Equations*. Springer: Berlin, 1986. Theory and algorithms.
5. Stenberg R. Analysis of mixed finite elements methods for the Stokes problem: a unified approach. *Mathematics of Computation* 1984; **42**(165):9–23.

